Available online at www.sciencedirect.com
SCIENCE DIRECT®
Journal of Solid State Chemistry 178 (2005) 3631–3638
JOURNAL OF SOLID STATE CHEMISTRY
www.elsevier.com/locate/jssc

The two-phase region in $2(ZnSe)_x(CuInSe_2)_{1-x}$ alloys and structural relation between the tetragonal and cubic phases

G. Wagner[a,*], S. Lehmann[a], S. Schorr[a], D. Spemann[b], Th. Doering[a]

[a]*Institute of Mineralogy, Crystallography and Materials Science, University of Leipzig, Scharnhorststr. 20, 04275 Leipzig, Germany*
[b]*Faculty for Physics and Earth Science, Nuclear Solid State Physics, University of Leipzig, Linnéstr. 5, D-04103 Leipzig, Germany*

Received 5 April 2005; received in revised form 8 September 2005; accepted 9 September 2005
Available online 2 November 2005

Abstract

The two-phase region in the system $2(ZnSe)_x(CuInSe_2)_{1-x}$ covers the chemical composition range $0.10 < x \leqslant 0.36$, in which a tetragonal and a cubic phase are coexisting. The structural relation between both phases was determined by selected area diffraction (SAD) and transmission electron microscopy (TEM). Both crystal structures are very similar and the extremely small mismatch of the lattice constants of the tetragonal phase and the embedding cubic matrix phase allows for the grain boundaries to be virtually strain-free and, therefore, without notable dislocations. The tetragonal phase forms grains of flat discus-like shape in the ambient cubic matrix, with the short discus axis parallel to the tetragonal **c**-axis. TEM experiments proved that the discus-shaped tetragonal particles are collinear with the $(100)_{cub}$, $(010)_{cub}$ and $(001)_{cub}$ planes of the cubic phase. Cooling and annealing experiments revealed a near-equilibrium state only to be realized for small cooling rates less than 2 K/h and/or for a long-time annealing with subsequent rapid quenching. Only then there will be no cation ordering in both, the tetragonal domains and the parental cubic matrix phase. If, however, the samples are kept in a state far away from the equilibrium condition both phases reveal Stannite-type cation ordering. Within the composition range of $0 \leqslant x \leqslant 0.10$ only tetragonal $2(ZnSe)_x(CuInSe_2)_{1-x}$-alloys exist. At concentration rates above 36 mol% 2(ZnSe) only cubic structured solid solutions of ZnSe and $CuInSe_2$ are found to be stable. However, in the range 36 mol% to about 60 mol% 2(ZnSe) tiny precipitates with Stannite-like structure exist, too.

Keywords: Phase diagram; Electron microscopy; $ZnSe/CuInSe_2$ alloys

1. Introduction

$CuInSe_2$ has been well-known for its potential of photovoltaic applications [1] for quite some time. In particular, expanding the band gap by alloying $CuInSe_2$ with $CuGaSe_2$ has improved the properties of photovoltaic devices [2,3], remarkably. By analogy with the 2ZnS–$CuInS_2$ system [4], the electronic band gap at room temperature may be expected to vary from $E_g(ZnSe) = 2.73$ eV [5] to $E_g(CuInSe_2) = 1.02$ eV [1] with the effect of the concentration ratio of 2(ZnSe) in $CuInSe_2$. Some first results reported by Gremenok et al. [6–8] have confirmed this idea. Hence, such alloys can expand the range of the commonly used materials for absorbers and/or buffers in thin film solar cells. However, for the system $2(ZnSe)_x(CuInSe_2)_{1-x}$ there is only a very narrow composition range between $0.31 < x \leqslant 0.36$ or $0.43 \leqslant x \leqslant 0.48$ (cf. Table 1) for the two phases with tetragonal and cubic structure to coexist. This means, there is a bit of a confusion about the two-phase cohabitation range and its temperature dependence. Moreover, there is little or no sound knowledge about the nature, morphology and segregation behaviour of the two phases. The aim of this paper is to present new results, namely about the crystallography, nucleation, growth behaviour, morphology and the domain or grain sizes of the second tetragonal phase. Emphasis is given to the two-phase cohabitation range at room temperature and the temperature dependence of the

*Corresponding author. Faculty of Chemistry and Mineralogy, Institute of Mineralogy, Crystallography and Materials Science, University of Leipzig, Linnéstr. 3-5 (TA), D-04103 Leipzig, Germany.
Fax: +49 341 97 36 249.
E-mail address: wagner@chemie.uni-leipzig.de (G. Wagner).

0022-4596/$ - see front matter © 2005 Elsevier Inc. All rights reserved.
doi:10.1016/j.jssc.2005.09.009

coexistence boundaries between the two phases has been determined within the subsolidus region in the system $2(ZnSe)_x(CuInSe_2)_{1-x}$. As shown later, our results deviate considerably from the literature data [9–13].

2. Experimental

To investigate the nucleation and the growth of the tetragonal phase (domains) within their embedding cubic matrix and to determine the extension of the two-phase coexistence field in the phase diagram we have adopted a two-fold strategy:

(1) Pre-synthesized (pre-annealing at 900 °C, 119 days) samples of nominal compositions of $Zn_{0.10}Cu_{0.45}In_{0.45}Se$ and $Zn_{0.30}Cu_{0.35}In_{0.35}Se$ were sealed in evacuated quartz ampoules and heated up at a rate of 10 K/h to 900 °C for 7, 9 or 10 days in order to establish the cubic phase of the alloy. The procedure of the pre-synthesis is described in more detail in Ref. [8]. Then, the samples were cooled down to room temperature at controlled cooling rates of $dT/dt = 2$, 5, 10, 15 and 42 K/h (cf. Table 2). To avoid the loss of selenium while annealing was in progress, the residual volume inside the ampoules was filled-up with a bulk quartz cylinder. These experiments yield nucleation and the growth rate data of the tetragonal domains.
(2) Pre-synthesized samples (pre-annealing at 850 °C, 39 and 40 days) of nominal compositions $Zn_{0.04}Cu_{0.48}In_{0.48}Se$, $Zn_{0.05}Cu_{0.475}In_{0.475}Se$, $Zn_{0.08}Cu_{0.46}In_{0.46}Se$, $Zn_{0.10}Cu_{0.45}In_{0.45}Se$, $Zn_{0.15}Cu_{0.425}In_{0.425}Se$ and $Zn_{0.25}Cu_{0.375}In_{0.375}Se$ were heated up to 850 °C at a rate of 10 K/h, then annealed for 12 days before they were cooled at a rate of 10 K/h down to the final annealing temperatures that are given in Table 3; T_{hom} is the temperature and t[d] the duration (in days) of that final annealing. This long-time annealing process was introduced to achieve a near-equilibrium state in concentration and growth of the domains and matrix phase. Eventually the samples were quenched in ice-water. Samples treated in such a way have been employed to determine the T–x-coexistence lines limiting the two-phase coexistence range.

Transmission electron microscopy (TEM) samples were prepared from the as-synthesized polycrystalline compact material by means of mechanical grinding and, polishing by Ar^+ ion thinning. Typical ion milling parameters were a 4 kV electric voltage, 0.5 mA beam current and an incident beam angle between 11° and 13°. The TEM and high-resolution TEM (HRTEM) were performed using a Philips CM 200 STEM with super twin objective lens (point resolution 0.23 nm). To identify those diffraction spots originating from cation ordering, SAD patterns for the different structures, with and without cation ordering, were simulated using the EMS-software package [14]. The average chemical composition of the samples and the specific compositions of the tetragonal domains and cubic matrix were measured by EDX-analysis in the STEM. A large beam diameter was used to determine the average sample composition. To precisely measure the particular compositions of the small domains and the surrounding

Table 1
Literature data on the two-phase coexistence range in the system $2(ZnSe)_x(CuInSe_2)_{1-x}$

Tetragonal phase (chalcopyrite structure)	Two-phase field	Cubic phase (sphalerite structure)	Remarks	Ref.
$0 \leqslant x < 0.31$	$0.31 \leqslant x \leqslant 0.36$	$0.36 < x \leqslant 1$	At about 550 °C	[9,10]
$0 \leqslant x < 0.43$	$0.43 \leqslant x \leqslant 0.48$	$0.48 < x \leqslant 1$		[11], see also [12,13]
$0 \leqslant x \leqslant 0.10$	$0.10 < x \leqslant 0.36$	$0.36 < x \leqslant 1$	At room temperature	This work

Table 2
Annealing temperature and time, cooling rate and chemical compositions for TEM-EDX measurements

Nominal 2(ZnSe) content (mol%)	T_{hom} (°C)	t_{hom} (days)	Cooling rate (K/h)	Average chemical composition TEM-EDX	Composition of tetragonal phase (domains)	Composition of cubic phase (matrix)
30	900	10	2	$Zn_{0.294}Cu_{0.335}In_{0.369}Se$	n.d.	n.d.
30	900	10	5	$Zn_{0.295}Cu_{0.334}In_{0.372}Se$	n.d.	n.d.
30	900	10	10	$Zn_{0.285}Cu_{0.338}In_{0.377}Se$	n.d.	n.d.
30	850	9	10	$Zn_{0.291}Cu_{0.334}In_{0.376}Se$	$Zn_{0.145}Cu_{0.392}In_{0.463}Se$	$Zn_{0.352}Cu_{0.306}In_{0.342}Se$
33	800	7	10	$Zn_{0.314}Cu_{0.337}In_{0.349}Se$	n.d.	$Zn_{0.347}Cu_{0.306}In_{0.347}Se$
30	900	10	15	$Zn_{0.288}Cu_{0.332}In_{0.381}Se$	n.d.	n.d.
30	900	7	42	$Zn_{0.275}Cu_{0.350}In_{0.374}Se$	n.d.	n.d.

n.d. means the chemical composition could not be detected because of too small domain sizes and their mutual overlapping (extremely high domain density). In that case it was not possible to determine the cubic phase composition, too. Their size, however, could be determined by TEM.

Table 3
Annealing temperature and time as well as chemical compositions as measured by means of TEM-EDX

T_{hom} (°C)	Nominal 2(ZnSe) content (mol%)	t_{hom} (days)	Average chemical composition TEM-EDX	Composition of tetragonal phase (domains)	Composition of cubic phase (matrix)
850	0	6	$Cu_{0.485}In_{0.520}Se_{0.994}$ (t)		—
850	10	21	$Zn_{0.097}Cu_{0.459}In_{0.444}Se$ (c)	Streaks, n.d.	$Zn_{0.097}Cu_{0.459}In_{0.444}Se$
800	25	21	$Zn_{0.237}Cu_{0.378}In_{0.385}Se$ (c)	Streaks, n.d.	$Zn_{0.237}Cu_{0.378}In_{0.385}Se$
750	4	74	$Zn_{0.047}Cu_{0.460}In_{0.499}Se$ (t)		No cubic phase
750	8	74	$Zn_{0.079}Cu_{0.459}In_{0.462}Se$	$Zn_{0.060}Cu_{0.459}In_{0.481}Se$	$Zn_{0.192}Cu_{0.400}In_{0.411}Se$
650	15	10	$Zn_{0.148}Cu_{0.419}In_{0.434}Se$	$Zn_{0.124}Cu_{0.412}In_{0.464}Se$	$Zn_{0.163}Cu_{0.404}In_{0.433}Se$
650	25	10	$Zn_{0.240}Cu_{0.379}In_{0.382}Se$ (c)	Streaks, n.d.	$Zn_{0.240}Cu_{0.379}In_{0.382}Se$
610	15	40	$Zn_{0.150}Cu_{0.408}In_{0.442}Se$ (c)	$Zn_{0.086}Cu_{0.429}In_{0.484}Se$	$Zn_{0.186}Cu_{0.380}In_{0.433}Se$
610	25	40	$Zn_{0.232}Cu_{0.356}In_{0.412}Se$ (c)	Streaks, n.d.	$Zn_{0.232}Cu_{0.356}In_{0.412}Se$
600	25	22	$Zn_{0.238}Cu_{0.373}In_{0.388}Se$ (c)	Streaks, n.d.	$Zn_{0.238}Cu_{0.373}In_{0.388}Se$
450	15	73		$Zn_{0.105}Cu_{0.385}In_{0.511}Se$	$Zn_{0.262}Cu_{0.307}In_{0.432}Se$
450	25	73	$Zn_{0.243}Cu_{0.353}In_{0.397}Se$	$Zn_{0.120}Cu_{0.411}In_{0.469}Se$	$Zn_{0.294}Cu_{0.329}In_{0.376}Se$
400	15	70	$Zn_{0.156}Cu_{0.410}In_{0.435}Se$	$Zn_{0.105}Cu_{0.425}In_{0.470}Se$	$Zn_{0.319}Cu_{0.319}In_{0.363}Se$
350	15	68		$Zn_{0.114}Cu_{0.395}In_{0.491}Se$	$Zn_{0.335}Cu_{0.320}In_{0.377}Se$

All samples were quenched after long-time annealing. "streaks, n.d." means the chemical composition could not be detected because of too small domain sizes (less than 10 nm) and their mutual overlapping (extremely high domain density). The presence of these tiny domains causes diffuse scattering in electron diffraction represented by streaks in the diffraction patterns. These streaks occur at positions characteristic of a tetragonal phase. In this case it was not possible to determine precisely the composition of the cubic phase too. Therefore, it is assumed that the average composition should be approximately equal to that of the cubic phase (c). (t) means that the sample consists solely of tetragonal material. If no average composition is quoted, then because of the very inhomogeneous distribution of both phases.

matrix the spot diameter was reduced to about 5–10 nm (nano-probe mode). Of course, the EDX-system was calibrated prior to all experiments. This means, the Cliff–Lorimer factors k_{AB} have been determined by means of standard samples, such as stoichiometric ZnSe, Cu_2Se, In_2Se_3 and $CuInSe_2$, respectively. The careful EDX-calibration allowed the Zn-concentration to be determined with an accuracy of ± 0.5 at%. To ensure this level of accuracy for all other results, the outcome of 12–15 individual local measurements of the composition parameters of the matrix and domains as well as the composition values obtained from overall integral measurements were averaged before finally compiled in Tables 2, 3 and 5.

The lattice parameters were determined by X-ray measurements on a Seifert XRD 3003-diffractometer using CuK_α radiation ($\lambda = 1.5418$ Å) and a secondary graphite monochromator. To correct the sample displacement error and the zero shift of the X-ray diffraction measurements, GaAs or Si were added to serve as an internal standard probe. The lattice parameters of single-phase samples were calculated from the whole powder diffraction pattern with the APX63 software package [15].

3. Results and discussion

3.1. Orientation relationship between tetragonal domains and cubic matrix

Grains inside the polycrystalline $2(ZnSe)_x(CuInSe_2)_{1-x}$ specimens, which are in (110), (100), (010) and (001) orientations, were selected to determine the orientation relationship between the tetragonal domains (α-phase) and the cubic phase matrix (β-phase). The tetragonal domains always appear as a part of a discus, that aligned in a grid-like rectangular pattern (see Fig. 1). The sample shown in Fig. 1 represents one in a near-equilibrium state (due to long-time annealing). It appears that the regions between the visible large domains are virtually free of any smaller ones. If, however, the samples are in a non-equilibrium state, then again a rectangular grid of large domains (called type-A) is formed but between these large domains many much smaller ones (named type-B) of the same chemical composition and orientation are found. This looks similar to the morphology found in the two-phase region of the $2(ZnS)_x(CuInS_2)_{1-x}$ system [16]. It seems that under equilibrium conditions the small domains gradually dissolve and eventually disappear all together. Then, as seen in Fig. 1, large domains of type A become dominant and only some small amount of type B-domains residue (some examples are marked in Fig. 1).

As confirmed by selected area diffraction (SAD), the tetragonal **c**-axis aligns always with the short axis of the discus and the tetragonal **a**- and/or **b**-axis lie parallel to its long axis (cf. Fig. 1).

Comparing the contrasts caused by the domains in (001), (100), (010) and (110) oriented grains, the flat discus-like bodies of the tetragonal phase (t) have to be arranged parallel to the (001)c, (100)c and (010)c planes of the cubic matrix (c) as depicted schematically in Fig. 2.

3.2. Growth behaviour of domains

To gain more information on the growth behaviour of the tetragonal domains, the same samples (average 2(ZnSe) content about 30 mol%) that were subjected to a controlled

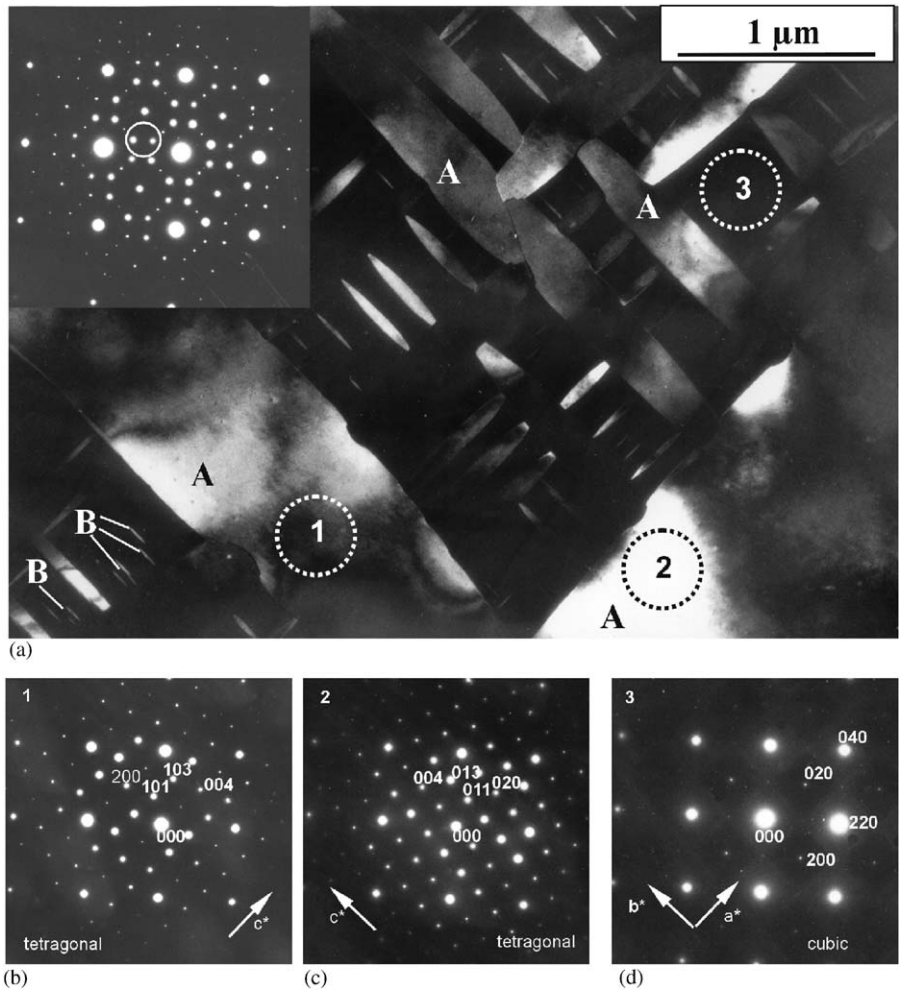

Fig. 1. (a) TEM dark-field image of tetragonal domains (1 and 2) and cubic matrix (3). Beam direction close to bd = [001]. The reflections used for imaging are encircled in the SAD pattern (see inset above). The average 2(ZnSe) content of the sample annealed at 350 °C is about 15 mol%, that of the tetragonal phase is $Zn_{0.114}Cu_{0.395}In_{0.491}Se$ and the cubic matrix consists of $Zn_{0.335}Cu_{0.320}In_{0.377}Se$. (b) The SAD diagram (1) results from the domain 1. (c) The SAD diagram (2) is obtained from domain 2 only. The SAD (3) shown in (d) originates entirely from the cubic matrix. The SAD pattern shown as inset in (a) is formed by superimposing of all three patterns. Due to long annealing time (see Table 2) this sample is in near-equilibrium state and, therefore, additional reflections caused by cation ordering are missing. The meaning of A and B is explained in the text.

cooling (cf. Table 2) have been examined by TEM dark-field observation. The length of the domains was measured on the micrographs (see Fig. 3). These values and, in addition, the time of domain growth are given in Table 4. Fig. 5 (phase diagram) indicates the domain nucleation to commence at temperatures of $T = 555\,^{\circ}C$ and to stall at $T = 300\,^{\circ}C$. Thus, the time for the domains to grow equals the cooling time through this temperature range of $\Delta T = 255\,K$ for the various cooling rates. According to Fig. 4, the growth of domains should be driven by diffusion ($\sim t^{1/2}$) just as for the sulphide system [16]. The dotted lines in Fig. 4 fit to the expected $C_g t^{1/2}$ dependence, where C_g is the average growth rate constant considering both the nucleation and growth. Its value is found to be about $1.86\,nm/min^{1/2}$ for the length and $0.31\,nm/min^{1/2}$ for the width within the temperature range of 555 and 300 °C and for the given average sample composition of 30 mol% 2(ZnSe) in $2(ZnSe)_x(CuInSe_2)_{1-x}$. Hence, the growth constant differs for the lateral (width of domains) and longitudinal (length of domains) growth. For temperatures $<300\,^{\circ}C$ the diffusion is assumed to be too slow for a remarkable domain growth, i.e. the growth of domains is completed.

3.3. Phase diagram

Based on the data given in Table 3 we can complete the phase diagram by the lines defining the two-phase coexistence area (see Fig. 5). These results are considerably different from those reported in the literature (cf. Table 1). Apparently, the DTA method (differential thermo-analysis) used there to determine the coexistence lines is inadequate, because the phase separation that leads to the formation of domains is diffusion driven and takes too long a time to complete. Therefore, a correct interpretation of DTA data must be doubted. However, we are quite sure

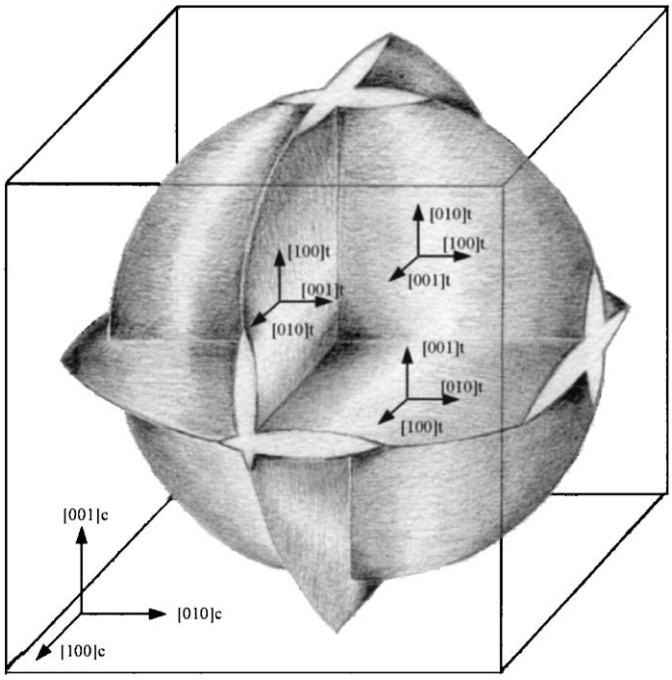

Fig. 2. Schematically drawn orientations of the discus-shaped tetragonal domains within their embedding cubic matrix (made by [21]).

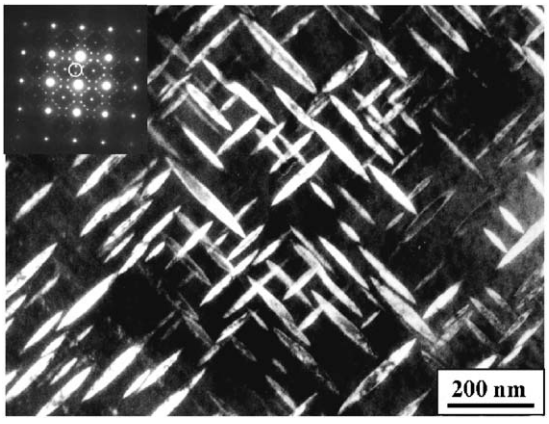

Fig. 3. TEM dark-field image from the reflections encircled in the SAD pattern (see inset). The average composition of the sample is $Zn_{0.294}Cu_{0.335}In_{0.369}Se$. The cooling rate was 2 K/h.

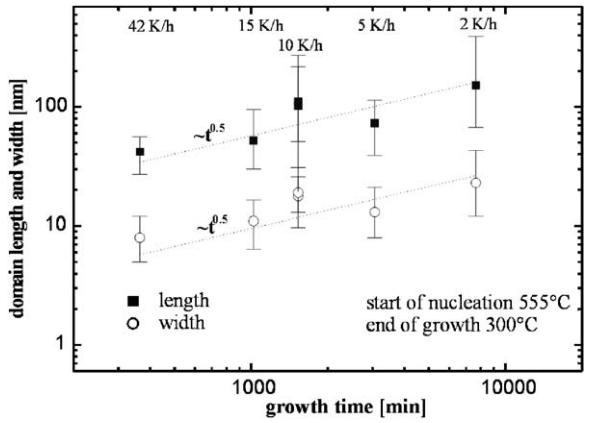

Fig. 4. Domain length versus growth time (length of stay). The average 2(ZnSe) content of all samples under consideration was about 30 mol%.

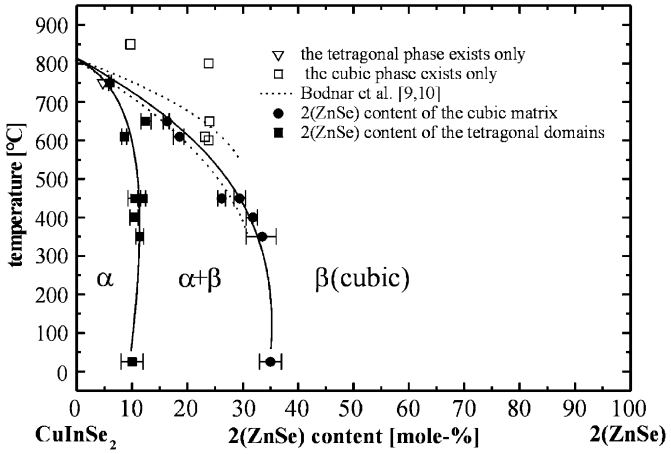

Fig. 5. TEM-EDX determined range of the two-phase region for different temperatures (terminated by full lines). The temperatures have an error of ± 10 K. The bold squares represent the composition of the tetragonal phase and the bold circles that of the cubic one. The two-phase coexistence area is found between both dotted lines first as reported by [9,10].

Table 4
Domain length and width for different cooling rates

Cooling rate (K/h)	Time period (min)	Average length (nm)	Minimum length (nm)	Maximum length (nm)	Average width (nm)	Minimum width (nm)	Maximum width (nm)
2	7650	152	67	394	23	12	43
5	3060	73	39	114	13	8	21
10	1530	111	51	218	19	13	31
10	1530	102	31	272	17.8	25.8	9.7
15	1020	52	30	95	11	6.4	16.5
42	364	42	27	56	8	5	12

The average 2(ZnSe) content in the $2(ZnSe)_x(CuInSe_2)_{1-x}$ was always $x \approx 0.3$. All samples were annealed at 900 °C and then cooled down to room temperature at different cooling rates. The length of domains was measured by TEM, only. Domain growth starts at 555 °C. Due to hardly noticeable diffusion further growing is assumed to stall at 300 °C (see Fig. 5). Hence, the domain growth regime expands across $\Delta T = 255$ K controlled by specific cooling rates given in the table.

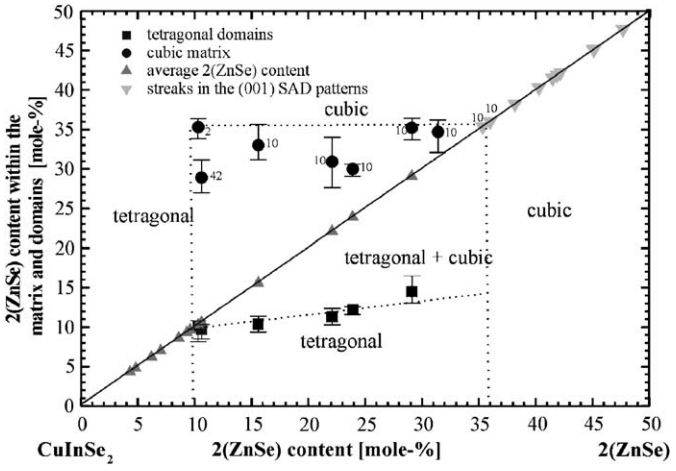

Fig. 6. TEM-EDX determined range of the two-phase region for room temperature. Note, the 2(ZnSe) concentration of the matrix approaches more and more the approximated equilibrium value (above dotted line) as the cooling rate decreases, cf. the sample close to 10 mol% 2(ZnSe). The numbers at the full circles are the applied cooling rates (in K/h).

of having determined the position of these phase boundary lines accurately within an error margin of ± 1 mol% 2(ZnSe) because the concentration measurement of individual domains and the matrix was performed independently and separately by TEM-EDX. The near-equilibrium compositions of the domains and matrix at room temperature were estimated from Fig. 6 using the data of Tables 2 and 5. Only the results of the cooling experiments were considered in Fig. 6. It should be noted that the 2(ZnSe) content deviates off the dashed line the more the cooling rate is increased. This is obvious for the matrix composition (cubic phase—β). Due to diffusion of mainly Cu and In towards the domains (tetragonal phase—α) the matrix composition has to be changed accordingly because remaining Zn stays within the matrix. Therefore, the matrix is gradually enriched with Zn, whereas the 2(ZnSe) content in the domains remains more or less constant for the various cooling rates. This result is reflected in the relatively weak domain scattering (bold squares in Fig. 6).

The reason for the large 2(ZnSe) concentration in the domains as shown in Fig. 5 at about 650 °C cannot be explained for sure. Perhaps, this effect may be caused by the existence of another yet unknown phase or a non-equilibrium state in the sample. A similar behaviour has been observed for the sulphide system, too [16].

In the following the composition range for 2(ZnSe) between $0.36 \leqslant x \leqslant 1$ is discussed only. As to be concluded from Table 5 and Fig. 5 (for >36 mol% 2(ZnSe) in $2(ZnSe)_x(CuInSe_2)_{1-x}$) these samples are free of any larger domains as shown in Figs. 1 and 3. However, within the SAD patterns, streaks (or diffuse reflection lines) appear which pass through positions that can be expected for diffraction spots from a tetragonal phase, possibly Stannite. It was impossible to determine the chemical composition of these extremely small domains (length less than about 10 nm). The simulation of SAD patterns from a Stannite-like structure (here $Zn_2CuInSe_4$ space group $I\bar{4}2m$) provides the reflections exactly at these positions. Since the observed domains (Fig. 7) are extremely thin (about 5 nm) the diffraction spots degenerate to streaks (inset in Fig. 7). They appear for 2(ZnSe) contents between 36 mol% and approximately 60 mol%. Strictly speaking, the Stannite structure, i.e. $(ABD_2)_{1-x}(CD)_{2x}$, is defined exactly at $x = 0.5$. At this composition a cubic phase has an ideal fcc lattice structure with each site of single occupancy by either atom A, B or C. Thus, a cation ordered Stannite phase is to be expected for the specific composition $x = 0.5$. At any higher 2(ZnSe) content (>60 mol%) the cubic phase is free of any other phases and no diffraction spots and/or streaks are observed in the SAD patterns. Hence, the appearance of the additional reflections in the diffraction patterns proves the existence of a tetragonal phase like Stannite which was theoretically predicted by Newman and Xiang [17], Osório et al [18] as well as Ni and Iwata [19]. According to their predictions this Stannite-type phase should be metastable in the composition range under consideration. This is confirmed with our experimental results; however, this phase appears to be more pronounced in rapidly cooled non-equilibrium state samples (cf. Fig. 7).

3.4. Lattice parameters

The lattice parameters of $2(ZnSe)_x(CuInSe_2)_{1-x}$ single-phase powder samples are determined from X-ray and neutron [20] powder diffraction measurements (Fig. 8). It was found that within the single-phase regions of the solid solution series the lattice parameters follow Vegard's rule, i.e. they depend linearly on the chemical composition (more details see [20]). By alloying $CuInSe_2$ into 2(ZnSe) the cubic lattice parameter a_{cub} increases because the atomic radii are $r_{In^{3+}} > r_{Zn^{2+}}$ whereas $r_{Cu^+} \cong r_{Zn^{2+}}$. On the other hand, by alloying 2(ZnSe) into $CuInSe_2$ the tetragonal lattice parameters a_{tet} and c_{tet} decrease with increasing 2(ZnSe) content.

4. Summary

The two-phase region in the system $2(ZnSe)_x(CuInSe_2)_{1-x}$ was investigated in the chemical composition range $0.10 < x \leqslant 0.36$. In this composition range a tetragonal and a cubic phase coexist. Because of their related crystal structures and the extremely small misfit between the tetragonal phase and the embedding cubic matrix their interfaces are nearly strain-free and, therefore, without any dislocations. The tetragonal phase which grows from the cubic matrix during the phase separation remains embedded into the cubic matrix and has the shape of a flat discus. The short extension of the discus is parallel to the tetragonal **c**-axis. TEM experiments proved that the discus-like particles have a tetragonal structure and are aligned

Table 5
Chemical composition of domains and matrix for different average compositions and cooling rates

Nominal 2(ZnSe) content (mol%)	T_{hom} (°C)	t_{hom} (days)	Cooling rate (K/h)	Average chemical composition WDX; PIXE/RBS*	Average chemical composition TEM-EDX	Tetragonal phase (domains) TEM-EDX	Cubic phase (matrix) TEM-EDX
4	850	21	2		$Zn_{0.043}Cu_{0.483}In_{0.475}Se$ (t)		no cubic phase
5	800	7	2		$Zn_{0.062}Cu_{0.410}In_{0.529}Se$ (t)		no cubic phase
5	850	21	2		$Zn_{0.048}Cu_{0.441}In_{0.512}Se$ (t)		no cubic phase
8	850	21	2		$Zn_{0.070}Cu_{0.452}In_{0.478}Se$ (t)		no cubic phase
10	900	7	2		$Zn_{0.103}Cu_{0.432}In_{0.466}Se$	$Zn_{0.101}Cu_{0.409}In_{0.491}Se$	$Zn_{0.353}Cu_{0.291}In_{0.357}Se$
10	900	7	5		$Zn_{0.086}Cu_{0.445}In_{0.470}Se$ (t)		no cubic phase
10	900	7	10		$Zn_{0.093}Cu_{0.434}In_{0.474}Se$ (t)		no cubic phase
10	900	119	42	$Zn_{0.098}Cu_{0.417}In_{0.486}Se$	$Zn_{0.106}Cu_{0.422}In_{0.472}Se$	$Zn_{0.097}Cu_{0.437}In_{0.467}Se$	$Zn_{0.289}Cu_{0.326}In_{0.383}Se$
10	850	9	10	$Zn_{0.101}Cu_{0.452}In_{0.463}Se_{1.031}$*	$Zn_{0.096}Cu_{0.430}In_{0.475}Se$ (t)		no cubic phase
15	800	7	10	$Zn_{0.148}Cu_{0.424}In_{0.442}Se_{0.985}$*	$Zn_{0.156}Cu_{0.411}In_{0.432}Se$	$Zn_{0.104}Cu_{0.426}In_{0.470}Se$	$Zn_{0.330}Cu_{0.316}In_{0.352}Se$
20	800	7	10	$Zn_{0.201}Cu_{0.399}In_{0.414}Se_{0.986}$*	$Zn_{0.221}Cu_{0.381}In_{0.393}Se$	$Zn_{0.113}Cu_{0.438}In_{0.449}Se$	$Zn_{0.309}Cu_{0.336}In_{0.356}Se$
25	800	7	10	$Zn_{0.250}Cu_{0.376}In_{0.390}Se_{0.984}$*	$Zn_{0.239}Cu_{0.372}In_{0.389}Se$	$Zn_{0.122}Cu_{0.427}In_{0.451}Se$	$Zn_{0.300}Cu_{0.337}In_{0.363}Se$
28	800	7	10		$Zn_{0.354}Cu_{0.304}In_{0.342}Se$	streaks, n.d.	
30	850	9	10	$Zn_{0.301}Cu_{0.362}In_{0.341}Se_{0.996}$	$Zn_{0.291}Cu_{0.334}In_{0.376}Se$	$Zn_{0.145}Cu_{0.392}In_{0.463}Se$	$Zn_{0.352}Cu_{0.306}In_{0.342}Se$
33	800	7	10	$Zn_{0.333}Cu_{0.339}In_{0.339}Se_{0.989}$*	$Zn_{0.314}Cu_{0.337}In_{0.349}Se$	n.d.	$Zn_{0.347}Cu_{0.306}In_{0.347}Se$
36	850	9	10	$Zn_{0.367}Cu_{0.321}In_{0.312}Se_{0.999}$	$Zn_{0.382}Cu_{0.291}In_{0.318}Se$	Streaks, n.d.	
36	850	9	10		$Zn_{0.415}Cu_{0.280}In_{0.305}Se$	Streaks, n.d.	
36	850	9	10		$Zn_{0.419}Cu_{0.283}In_{0.298}Se$	Streaks, n.d.	
40	850	9	10	$Zn_{0.389}Cu_{0.310}In_{0.301}Se_{1.0}$	$Zn_{0.360}Cu_{0.293}In_{0.347}Se$	Streaks, n.d.	
42	800	7	10		$Zn_{0.403}Cu_{0.287}In_{0.311}Se$	Streaks, n.d.	
44	800	7	10	$Zn_{0.447}Cu_{0.279}In_{0.293}Se_{0.982}$*	$Zn_{0.422}Cu_{0.275}In_{0.303}Se$	Streaks, n.d.	
46	800	7	10		$Zn_{0.502}Cu_{0.237}In_{0.261}Se$	Streaks, n.d.	
48	800	7	10	$Zn_{0.510}Cu_{0.283}In_{0245}Se_{0.961}$*	$Zn_{0.452}Cu_{0.279}In_{0.270}Se$	Streaks, n.d.	
48	800	7	10		$Zn_{0.451}Cu_{0.273}In_{0.275}Se$	Streaks, n.d.	
50	850	9	10	$Zn_{0.518}Cu_{0.251}In_{0237}Se_{0.993}$*	$Zn_{0.477}Cu_{0.247}In_{0.276}Se$	Streaks, n.d.	
55	800	7	10		$Zn_{0.525}Cu_{0.232}In_{0.241}Se$	Streaks, n.d.	
60	800	7	10		$Zn_{0.574}Cu_{0.208}In_{0.218}Se$	Streaks, n.d.	
70	800	7	10		$Zn_{0.675}Cu_{0.157}In_{0.168}Se$ (c)	No streaks	
80	800	7	10		$Zn_{0.797}Cu_{0.096}In_{0106}Se$ (c)	No streaks	
90	800	7	10		$Zn_{0.871}Cu_{0.064}In_{0.064}Se$ (c)	No streaks	
95	800	7	10		$Zn_{0.923}Cu_{0.036}In_{0.039}Se$ (c)	No streaks	

"streaks, n.d." means the chemical composition could not be detected because of too small domain sizes (less than 5 nm) and their mutual overlapping (extremely high domain density). The presence of these tiny domains causes diffuse scattering in electron diffraction represented by streaks in the diffraction pattern. These streaks occur at positions characteristic of a tetragonal phase. In this case it was not possible to determine precisely the composition of the cubic phase too. Therefore, it is assumed that the average composition should be approximately equal to that of the cubic phase (c). (t) means that the sample consists solely of tetragonal material.

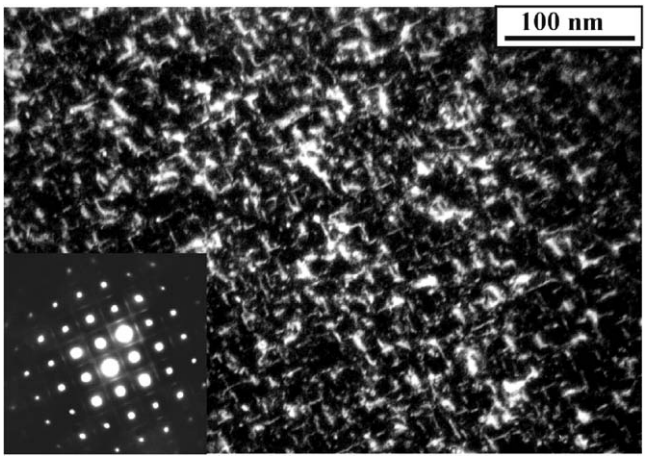

Fig. 7. TEM dark-field image of extremely small "domains" of Stannite-like structure. The average composition of the sample is $Zn_{0.382}Cu_{0.291}In_{0.318}Se$ and the cooling rate was 10 K/h. Beam direction close to [001].

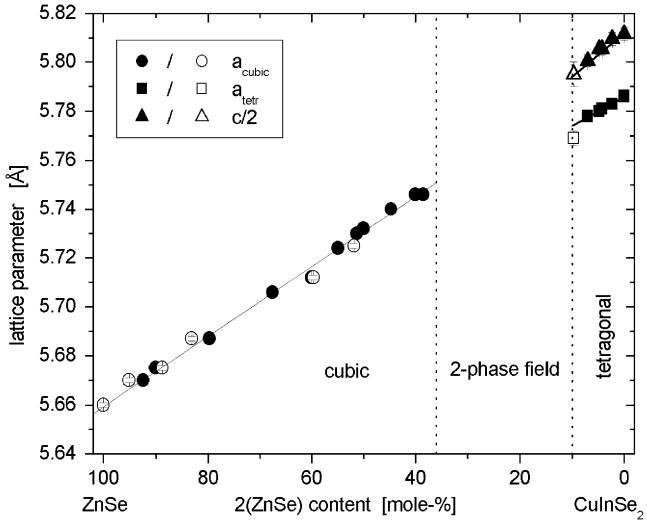

Fig. 8. Lattice parameters of $2(ZnSe)_x(CuInSe_2)_{1-x}$ single-phase samples versus chemical composition. Solid lines represent a linear fit to the data, dotted lines mark the two-phase field. Solid symbols refer to lattice parameters determined by neutron powder diffraction [20].

with the (100)c, (010)c and (001)c planes of the cubic matrix. Long-time annealing experiments followed by rapid quenching are suitable to prepare samples near to equilibrium concentrations. However, cooling experiments revealed a near-equilibrium state only to be realized for cooling rates <2 K/h. Then, the tetragonal domains as well as the embedding cubic matrix are free of cation ordering. If the samples are far away from the equilibrium state both phases are infected by Stannite-type cation ordering. Within the composition range $0 \leqslant x \leqslant 0.10$ only tetragonal $2(ZnSe)_x(CuInSe2)_{1-x}$ alloys exist. Generally, above 36 mol% 2(ZnSe) to pure ZnSe solid solutions of ZnSe and $CuInSe_2$ with Sphalerite-like structure are stable. However, in the range from 36 mol% to about 60 mol%, 2(ZnSe) tiny precipitates with Stannite-like structure exist as confirmed by the occurrence of streaks in the selected area diffraction patterns.

Acknowledgments

The authors would like to acknowledge Dr. Holger Tietze-Jaensch (Forschungszentrum Juelich GmbH, Institute for Safety Research and Reactor Technology) for critical reading of the manuscript and many constructive improvements. This work was financially supported by BMBF under contract 03WK108. Gratitude is also given to Mrs. Peter for preparing TEM samples.

References

[1] H. Neumann, $A^IB^{III}C_2^{VI}$ compounds as new optoelectronic materials, in: A. Hermann (Ed.), Optoelectronic Materials and Devices, Proceedings of the Third International School, Cetniewo (Poland), 1981, p. 171.
[2] U. Rau, H.W. Schock, Appl. Phys. A 69 (1999) 131.
[3] W.N. Shafarman, R. Klenk, B.E. McCandless, J. Appl. Phys. 79 (1996) 7324.
[4] I. Luck, W. Henrion, R. Scheer, Th. Doering, K. Bente, H.J. Lewerenz, Cryst. Res. Technol. 31 (1996) 841.
[5] S.V. Svechnikov, in $A^IB^{III}C_2^{VI}$ compounds as new optoelectronic materials, in: A. Hermann (Ed.), Optoelectronic Materials and Devices, Proceedings of the Third International School, Cetniewo (Poland), 1981, p.141.
[6] V.F. Gremenok, W. Schmitz, I.V. Bodnar, K. Bente, Th. Doering, G. Kommichau, I.A. Victorov, A. Eifler, V. Riede, in: Proceedings of the 12th International Conference on Ternary and Multinary Compounds; Jpn. J. Appl. Phys. 39 (Suppl. 39-1) (2000) 277.
[7] I.V. Bodnar, V.F. Gremenok, Inorg. Mater. 39 (2003) 1122.
[8] S. Lehmann, Undergraduate Dissertation, University Leipzig 2003.
[9] I.V. Bodnar, I.V. Chibusova, Russ. J. Inorg. Chem. 43 (1998) 1783.
[10] I.V. Bodnar, I.A. Victorov, I.V. Chibusova, Inst. Phys. Conf. Ser. 152 (1997) 119.
[11] J.N. Gan, J. Tauc, V.J. Lamprecht Jr., M. Robbins, Phys. Rev. B 12 (1975) 5797.
[12] P. Grima Gallardo, Phys. Stat. Sol. (a) 134 (1992) 119.
[13] P. Manca, L. Garbato, Solar Cells 16 (1986) 101.
[14] P.A. Stadelmann, Ultramicroscopy 21 (1987) 131.
[15] APX software, Freiberger Präzisionsmechanik.
[16] G. Wagner, F. Fleischer, S. Schorr, K. Bente, J. Cryst. Growth 283 (2005) 356.
[17] K.E. Newman, X. Xiang, Phys. Rev. B 44 (1991) 4677.
[18] R. Osório, Z.W. Lu, S.-H. Wei, A. Zunger, Phys. Rev. B 47 (1993) 9985.
[19] J. Ni, Sh. Iwata, Phys. Rev. B 52 (1995) 3214.
[20] S. Schorr, M. Tovar, D. Sheptyakov, L. Keller, G. Geandier, Structure and cation distribution of the solid solution series $2ZnX-CuInX_2$ (X = S, Se, Te), J. Phys. Chem. Solids, 2005, in press.
[21] L. Schubert, University Leipzig 2003, Hand-painted.